Disease Research Center, St. Louis, Missouri, United States; [21]Washington University, St. Louis, Missouri, United States. Contact e-mail: blazeyt@mir.wustl.edu

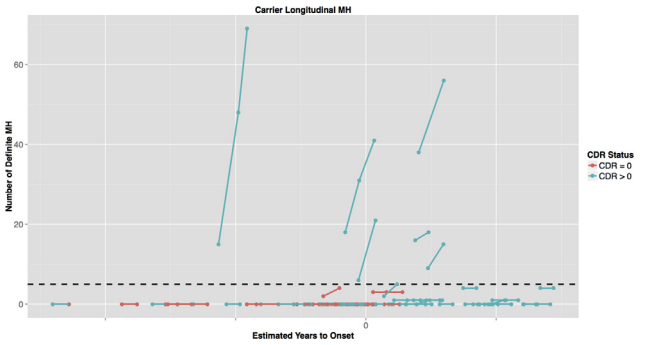

Table 1
MH contingency table separated by MH load and CDR status. (NC=Non-carrier, M+=Mutation Carrier)

# of MH	NC	M+/CDR=0	M+/CDR=0.5	M+/CDR>0.5	Total
0	91	80	26	16	213
1-4	5	5	5	4	19
>4	0	0	4	2	6
Total	96	85	35	22	238

Background: Cerebral microhemorrhages (MH), defined as small, hypointense lesions on T2/T2* weighted images, occur in approximately 23% of Alzheimer's disease (AD) cases. Furthermore, anti-amyloid treatment trials have been associated with the development of MHs . As a response to concerns about the safety of increased MH loads, the Alzheimer's Association Research Roundtable Workgroup recommended that individuals with more than 4 MHs be excluded from clinical trials. There is, however, only one extant in vivo study examining the prevalence of MH in autosomal dominant cases of AD (ADAD). With clinical trials of amyloid modifying agents soon to begin in ADAD populations, there is a pressing need to establish the prevalence of MH in this disease. **Methods:** Individuals from families with a history of ADAD were recruited at 11 sites worldwide, as part of the DIAN initiative. In total, 96 non-carriers (NC) and 142 carriers (M+) were studied. Longitudinal MH data was available for 25 non-carriers and 59 carriers. A 3T susceptibility-weighted imaging (SWI) sequence was used to quantify the number of MHs in each participant. Following the recommendation of Sperling et al., instances of siderosis were included along with MH counts. **Results:** Approximately 26% (15/57) of symptomatic (CDR>0) ADAD mutation carriers had at least one MH (Table 1). Of the 142 mutation carriers, only 6 had more than four MHs. None of these participants carried the Dutch (Glu693Gln or E693Q) mutation subtype. Within mutation carriers there was clear association with CDR: both the M+/CDR=0.5 and M+/CDR>0.5 groups had greater MH counts than the M+/CDR=0 group ($p<0.0001$). Longitudinal imaging revealed that individuals with more than 4 MH at baseline showed a dramatic increase in the number of MHs at follow-up (Figure 1). **Conclusions:** Rates for MHs in our study are similar to those reported in a recent meta-analysis in sporadic AD, and in a small study of ADAD mutation carriers. Only six of the participants in this study would have been excluded from a clinical trial due to MH load. Furthermore, no asymptomatic carriers met the MCH cutpoint, suggesting that pre-symptomatic trials in ADAD may not be overly burdened by current MH load recommendations.

IC-P-104 CHARACTERIZATION OF CORTICAL MICROSTRUCTURAL CHANGES IN ALZHEIMER'S DISEASE

Brian Gordon[1], **Tyler Blazey**[2], Samantha Allison[3], John Morris[2], Tammie Benzinger[4], Denise Head[2], *[1]Washington University in St. Louis, St. Louis, Missouri, United States; [2]Washington University, St. Louis, Missouri, United States; [3]Washington Univeristy, St. Louis, Missouri, United States; [4]Washington University, St. Louis, Missouri, United States. Contact e-mail: blazeyt@mir.wustl.edu*

Background: MRI in Alzheimer's disease (AD) has primarily measured declines in grey matter thickness and volume. There is a growing interest in understanding how both grey matter microstructure and myelination are altered in AD. Previous examinations of white matter have been restricted to large fiber bundles, whereas myelin is distributed throughout the cortex. We used the ratio of intensities in a T1-weighted image (T1w) to a T2-weighted (T2w) image (T1w/T2w, or Myelin Map) to evaluate grey matter microstructure and compared this to measurements of cortical thickness. **Methods:** Participants consisted of cognitively normal individuals (n=44, mean age=74.5) and a collapsed population of participants with very mild (n=31, CDR=0.5, mean age=78) and mild (n=12, CDR=1, mean age 77) AD. Cortical thickness was estimated using Freesurfer. Estimates of cortical myelination were generated using Caret (1). **Results:** Participants with dementia had widespread reductions in cortical thickness compared to controls (Figure 1). They had lower T1w/T2w ratios in primary sensory and motor cortices, which suggests a loss of cortical microstructure, likely due to demyelination. Conversely, the dementia group exhibited higher T1w/T2w ratios in the temporal lobe, medial prefrontal and cingulate cortex suggesting divergent pathological processes in those areas. **Conclusions:** This study represents a novel attempt to utilize T1w/T2w ratios to further define cortical microstructural changes in AD. Both the strength and direction of these effects appear to be regional in nature. (1) Glasser, M. F., & Van Essen, D. C. (2011). Mapping human cortical areas in vivo based on myelin content as revealed by T1- and T2-weighted MRI. The Journal of neuroscience: the official journal of the Society for Neuroscience, 31(32), 11597-616.

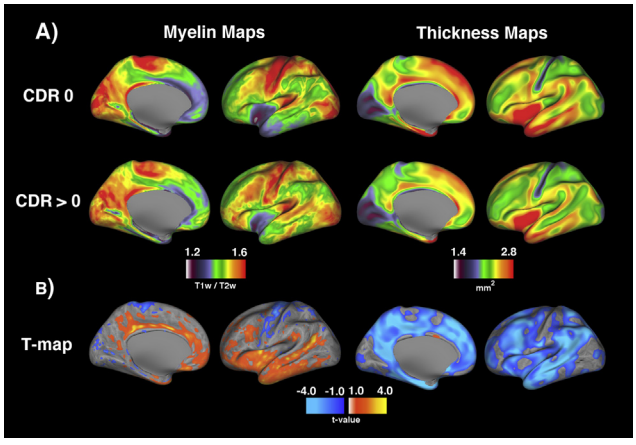

IC-P-105 SELF-REPORTED VERSUS INFORMANT-BASED COGNITIVE COMPLAINTS: RELATION OF E-COG SCORES TO IMAGING BIOMARKERS AND CLINICAL STATUS IN ADNI-2

Shannon Risacher[1], Ronald Petersen[2], Paul Aisen[3], Clifford Jack[2], Robert Koeppe[4], William Jagust[5], Sarah Tomaszewski Farias[6], Dan Mungas[7], John Trojanowski[8], Leslie Shaw[9], Michael Weiner[10], Andrew Saykin[1], *[1]Indiana University School of Medicine,*

	HC	E-MCI	L-MCI	AD	ANOVA/χ2 p
n	256	287	210	142	n/a
Age	75.3 (0.5)	71.0 (0.4)	73.8 (0.5)	75.7 (0.6)	p<0.001
Gender (M, F)	123, 133	162, 125	119, 91	86, 56	p=0.07
Education	16.4 (0.2)	16.0 (0.2)	16.3 (0.2)	15.9 (0.2)	ns
Handedness (R, L)	235, 21	258, 29	187, 23	129, 13	ns
CDR-Sum of Boxes	0.1 (0.1)	1.3 (0.1)	1.7 (0.1)	5.0 (0.2)	p<0.001
GDS Total Score	0.8 (0.1)	1.8 (0.1)	1.9 (0.1)	2.1 (0.1)	p<0.001
MMSE Total Score	29.0 (0.1)	28.3 (0.1)	27.6 (0.1)	22.4 (0.2)	p<0.001
Logical Memory – Immediate	14.6 (0.2)	11.0 (0.2)	8.1 (0.2)	4.1 (0.3)	p<0.001
Logical Memory – Delayed	13.7 (0.2)	9.0 (0.2)	5.1 (0.2)	1.6 (0.3)	p<0.001
Rey AVLT Total Score	45.4 (0.6)	39.2 (0.6)	33.3 (0.7)	23.1 (0.8)	p<0.001
Rey AVLT Delayed Score	7.5 (0.2)	5.7 (0.2)	3.3 (0.2)	1.0 (0.3)	p<0.001
ECog-Self: Memory (% endorsed)	44.3 (1.7)	75.2 (1.6)	78.5 (1.8)	81.5 (2.3)	p<0.001
ECog-Self: Language (% endorsed)	31.1 (1.9)	58.4 (1.8)	58.4 (2.1)	54.5 (2.7)	p<0.001
ECog-Self: Visuospatial (% endorsed)	11.6 (1.9)	32.1 (1.8)	32.7 (2.1)	42.2 (2.6)	p<0.001
ECog-Self: Organization (% endorsed)	13.2 (2.1)	36.4 (2.0)	40.5 (2.3)	45.6 (2.9)	p<0.001
ECog-Self: Planning (% endorsed)	22.9 (2.1)	41.0 (2.0)	42.7 (2.3)	47.1 (3.0)	p<0.001
ECog-Self: Divided Attention (% endorsed)	37.7 (2.3)	63.9 (2.2)	61.8 (2.5)	64.1 (3.3)	p<0.001
ECog-Self: Total (% endorsed)	27.3 (1.5)	52.1 (1.5)	53.6 (1.7)	56.9 (2.1)	p<0.001
ECog-Inf: Memory (% endorsed)	24.5 (1.7)	63.5 (1.6)	76.1 (1.8)	97.2 (2.3)	p<0.001
ECog-Inf: Language (% endorsed)	12.3 (1.8)	40.3 (1.7)	48.8 (2.0)	82.1 (2.4)	p<0.001
ECog-Inf: Visuospatial (% endorsed)	6.9 (1.8)	26.2 (1.7)	35.3 (1.9)	73.0 (2.4)	p<0.001
ECog-Inf: Organization (% endorsed)	9.9 (2.0)	33.7 (1.9)	46.0 (2.1)	83.7 (2.6)	p<0.001
ECog-Inf: Planning (% endorsed)	12.7 (2.0)	35.4 (1.9)	46.0 (2.2)	85.2 (2.7)	p<0.001
ECog-Inf: Divided Attention (% endorsed)	21.0 (2.3)	57.1 (2.2)	60.7 (2.5)	92.6 (3.0)	p<0.001
ECog-Inf: Total (% endorsed)	14.5 (1.5)	42.5 (1.4)	52.7 (1.6)	85.5 (2.0)	p<0.001
Mean Global Florbetapir SUVR	1.14 (0.01)	1.18 (0.01)	1.23 (0.01)	1.29 (0.01)	p<0.001
Mean Global FDG SUVR	1.37 (0.01)	1.36 (0.01)	1.32 (0.01)	1.25 (0.01)	p<0.001
Mean Hippocampal Volume	3831.0 (33.3)	3614.2 (26.5)	3326.5 (36.9)	3007.1 (47.9)	p<0.001
CSF A$\beta_{1\text{-}42}$	237.1 (7.0)	228.8 (5.2)	181.9 (8.7)	161.9 (15.0)	p<0.001
CSF Total Tau	69.6 (4.9)	83.0 (3.6)	103.2 (6.1)	130.4 (6.1)	p<0.001
CSF P-Tau	20.7 (1.1)	22.7 (0.8)	29.7 (1.4)	31.9 (2.3)	p<0.001

Indianapolis, Indiana, United States; [2]Mayo Clinic, Rochester, Minnesota, United States; [3]UCSD, La Jolla, California, United States; [4]University of Michigan, Ann Arbor, Michigan, United States; [5]University of California, Berkeley, Berkeley, California, United States; [6]University of California, Davis, Sacramento, California, United States; [7]UC Davis, Sacramento, California, United States; [8]University of Pennsylvania School of Medicine, Philadelphia, Pennsylvania, United States; [9]University of Pennsylvania Medical Center, Philadelphia, Pennsylvania, United States; [10]Center for Imaging of Neurodegenerative Diseases; VA Medical Center and UCSF, San Francisco, California, United States.
Contact e-mail: srisache@iupui.edu

Background: Cognitive complaints are common in older adults including controls with generally intact psychometric performance (HC) as well as those with early or late mild cognitive impairment (EMCI, LMCI). We analyzed the relationships between imaging biomarkers, clinical performance, and cognitive complaints on the Measurement of Everyday Cognition (E-Cog) from both the participant and his or her informant in the ADNI-2 cohort. **Methods:** Data from 895 participants were analyzed (256 HC, 287 EMCI, 210 LMCI, 142 AD). Measures of amyloid deposition, glucose metabolism, and brain atrophy from target regions of interest (ROIs) were extracted from Florbetapir PET, fluorodeoxyglucose (FDG) PET, and structural MRI, respectively. PET scans were processed using standard techniques to generate SUVR measures intensity normalized to the whole cerebellum (Florbetapir) and pons (FDG). MRI scans were analyzed using Freesurfer (R0Is) and SPM8 (voxel based morphometry). Clinical, diagnostic, CSF, and cognitive performance data was also obtained for all available participants at the first ADNI-GO/2 visit. Associations between amyloid deposition, glucose metabolism, brain atrophy, CSF A β and tau levels, cognitive performance, and the extent of cognitive complaints on the E-Cog from the participant and informant were assessed. **Results:** Diagnostic groups differed in E-Cog scores for both participants and informants as expected (Table 1), with greater complaints in the MCI and AD groups. Significant associations between E-Cog self and informant measures and cognitive performance, amyloid deposition, glucose metabolism, CSF A β and tau, and brain atrophy were also observed across the full sample and within diagnostic groups (Figure 1). Generally, informant E-Cog scores in the memory domain and across all cognitive domains showed more significant associations with biomarkers and clinical performance than self-ratings by the participant. A notable exception was depressive symptoms which were more significantly associated with self E-Cog scores than informant scores. **Conclusions:** Informant ratings of cognitive decline in mildly impaired and cognitively healthy participants are better predictors of cognitive performance and AD biomarker status than self-reported cognitive complaints. For very early detection of incipient cognitive decline in secondary prevention trials it may be advisable to ascertain informant ratings of apparently healthy older adults and not only in those suspected of MCI or dementia.

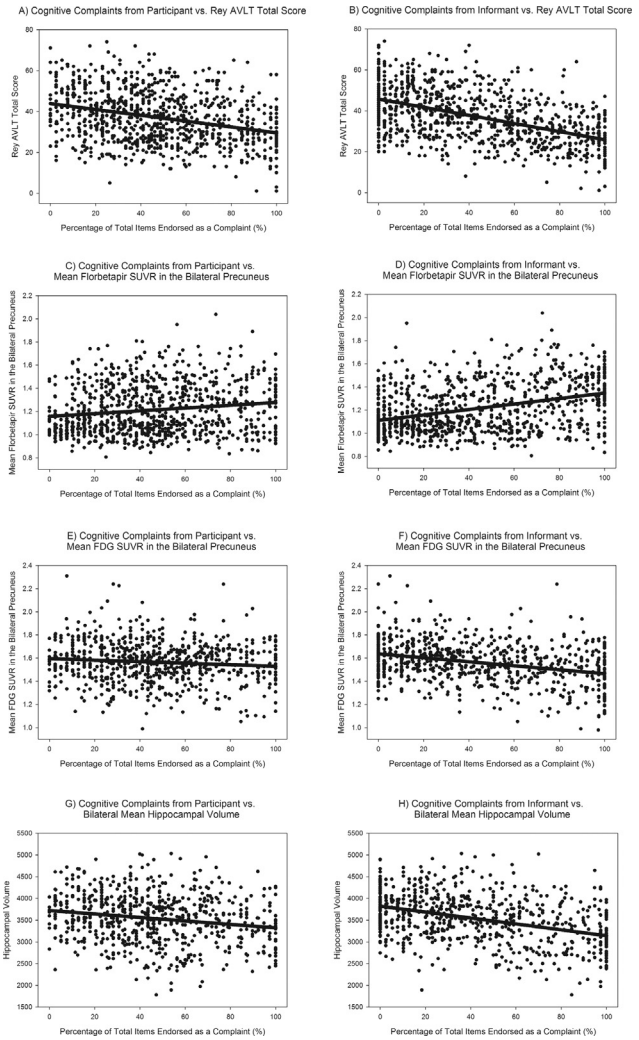

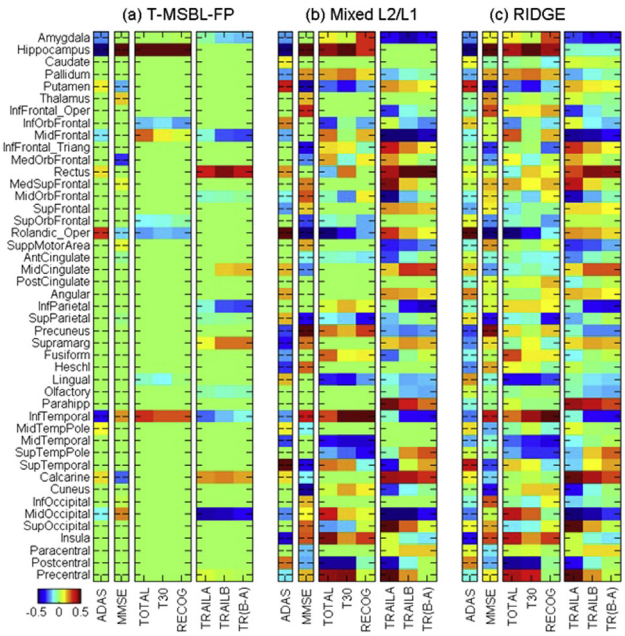

Figure 1. Heat maps of average regression weights of 5-fold cross-validation trials for (a) T-MSBL-FP, (b) the Mixed L2/L1, and (c) RIDGE regression. Each row corresponds to a MRI measure and each column corresponds to a cognitive score. Blue indicates negative correlation, while red indicates positive correlation. The bigger the value of a coefficient, the more important its VBM measure is in predicting the corresponding cognitive score.

Table 1
45 VBM measures

Region Group	VBM Grey Matter Density (45 in total)
Subcortical (temporal)	Amygdala, Hippocampus
Subcortical (striatum/basal ganglia)	Caudate, Pallidum, Putamen
Subcortical (thalamus)	Thalamus
Frontal Lobe	InfFrontal_Oper, InfOrbFrontal, MidFrontal, InfRrontal_Triang, MedOrbFrontal, Rectus, MedSupFrontal, MidOrbFrontal, SupFrontal, SupOrbFrontal, Rolandic_Oper, SuppMotorArea
Cingulate	AntCingulate, MidCingulate, PostCingulate
Parietal Lobe	Angular, InfParietal, SupParietal, Precuneus, Supramarg
Temporal Lobe (cortical)	Fusiform, Heschl, Lingual, Olfactory, Parahipp, InfTemporal, MidTempPole, MidTemporal, SupTempPole, SupTemporal
Occiptal Lobe	Calcarine, Cuneus, InfOccipital, MidOccipital, SupOccipital
Insula	Insula
Sensory-Motor Cortex	Paracentral, Postcentral, Precentral

IC-P-106 SPARSE BAYESIAN LEARNING FOR IDENTIFYING THE NEUROANATOMICAL BASIS OF COGNITIVE IMPAIRMENT IN ALZHEIMER'S DISEASE

Jing Wan[1], Zhilin Zhang[2], Shiaofen Fang[3], Shannon Risacher[4], Andrew Saykin[4], Li Shen[4] FOR THE ALZHEIMER'S DISEASE NEUROIMAGING INITIATIVE (ADNI)[5], *[1]Purdue University, Indianapolis, Indianapolis, Indiana, United States; [2]Samsung R&D America-Dallas, Richardson, Texas, United States; [3]Indiana University-Purdue University Indianapolis, Indianapolis, Indiana, United States; [4]Indiana University School of Medicine, Indianapolis, Indiana, United States; [5]UC San Francisco, San Francisco, California, United States. Contact e-mail: wanjing@iupui.edu*

Background: Multivariate regression model was employed for predicting multiple cognitive scores from MRI measures. A sparse Bayesian learning algorithm was applied to the ADNI database, which exploited dependence across the cognitive scores via explicitly modeling correlation among the regression coefficients. **Methods:** Data were obtained from the Alzheimer's Disease Neuroimaging Initiative (ADNI) database. 160 AD and 219 healthy control (HC) participants were included. The baseline 1.5T MRI scan of each participant was processed using voxel-based morphometry (VBM) in SPM5 [1]. The grey matter (GM) density of 45 AAL regions of interest (Table 1) from each hemisphere was extracted and the bilateral measures were averaged to generate one single measure for each structure. Four sets of cognitive scores [2] were examined as response variables: ADAS, MMSE, RAVLT and TRAILS. All the VBM measures and cognitive scores were pre-adjusted for baseline age, gender, education, and handedness. A sparse Bayesian learning algorithm, T-MSBL-FP [3], was adopted to predict cognitive scores from VBM data, and compared with Mixed L2/L1 minimization algorithm [3] and RIDGE Regression [3]. 5-fold cross validation method was used to obtain an unbiased estimate of prediction performance.